The Journal of Immunology

RESEARCH ARTICLE | DECEMBER 01 2010

CTL Induction of Tumoricidal Nitric Oxide Production by Intratumoral Macrophages Is Critical for Tumor Elimination FREE

Rodolfo D. Vicetti Miguel; ... et. al

J Immunol (2010) 185 (11): 6706–6718.
https://doi.org/10.4049/jimmunol.0903411

Related Content

Intratumoral Injection of CpG Oligonucleotides Induces the Differentiation and Reduces the Immunosuppressive Activity of Myeloid-Derived Suppressor Cells

J Immunol (February,2012)

Destructive and nondestructive patterns of immune rejection of syngeneic intraocular tumors.

J Immunol (June,1987)

Macrophage-mediated tumor cell killing: regulation of expression of cytolytic activity by prostaglandin E.

J Immunol (February,1981)

Downloaded from http://journals.aai.org/jimmunol/article-pdf/185/11/6706/1325334/0903411.pdf by guest on 20 April 2024

CTL Induction of Tumoricidal Nitric Oxide Production by Intratumoral Macrophages Is Critical for Tumor Elimination

Rodolfo D. Vicetti Miguel,[*,†,‡] Thomas L. Cherpes,[§] Leah J. Watson,[¶,1] and Kyle C. McKenna[†,‡]

To characterize mechanisms of CTL inhibition within an ocular tumor microenvironment, tumor-specific CTLs were transferred into mice with tumors developing within the anterior chamber of the eye or skin. Ocular tumors were resistant to CTL transfer therapy whereas skin tumors were sensitive. CTLs infiltrated ocular tumors at higher CTL/tumor ratios than in skin tumors and demonstrated comparable ex vivo effector function to CTLs within skin tumors indicating that ocular tumor progression was not due to decreased CTL accumulation or inhibited CTL function within the eye. $CD11b^+Gr\text{-}1^+F4/80^-$ cells predominated within ocular tumors, whereas skin tumors were primarily infiltrated by $CD11b^+Gr\text{-}1^-F4/80^+$ macrophages (Mϕs), suggesting that myeloid derived suppressor cells may contribute to ocular tumor growth. However, $CD11b^+$ myeloid cells isolated from either tumor site suppressed CTL activity in vitro via NO production. Paradoxically, the regression of skin tumors by CTL transfer therapy required NO production by intratumoral Mϕs indicating that NO-producing intratumoral myeloid cells did not suppress the effector phase of CTL. Upon CTL transfer, tumoricidal concentrations of NO were only produced by skin tumor-associated Mϕs though ocular tumor-associated Mϕs demonstrated comparable expression of inducible NO synthase protein suggesting that NO synthase enzymatic activity was compromised within the eye. Correspondingly, in vitro-activated Mϕs limited tumor growth when co-injected with tumor cells in the skin but not in the eye. In conclusion, the decreased capacity of Mϕs to produce NO within the ocular microenvironment limits CTL tumoricidal activity allowing ocular tumors to progress. ***The Journal of Immunology*****, 2010, 185: 6706–6718.**

Ocular immune privilege is an evolutionary adaptation that preserves vision by minimizing immunopathology during pathogen clearance (1, 2). Stringent immune regulation within the eye, however, can limit protective tumoricidal immune responses providing a permissive environment for tumor development and persistence (3). For example, limited numbers of certain immunogenic tumor cell lines are eliminated by tumor-specific $CD8^+$ CTL responses when injected in the skin but not in the anterior chamber (a.c.) of the eyes of mice (4, 5). Notably, progressive ocular tumor growth primes for tumor-specific CTLs (6, 7) capable of eliminating a subsequent tumor challenge in the skin or opposite eye, a phenomenon termed intracamerally induced concomitant immunity (8). These data indicate that CTLs can infiltrate the immune privileged eye and exert effector function but fail to demonstrate tumoricidal activity in established ocular tumors. Similarly, in some uveal melanoma patients, progressive primary ocular tumor development occurs despite pronounced infiltration by $CD8^+$ T cells (9, 10), which suggests that CTLs are primed and expanded in response to tumor Ags but are not capable of mediating their tumoricidal activity within the established ocular tumor microenvironment.

There are several potential explanations that alone or in combination may account for CTL inhibition within established ocular tumors. To begin, tumor development in the eye may preferentially generate tumor variants that are resistant to CTL responses (11, 12). In contrast, CTL activity could be inhibited by reducing the number of ocular tumor-infiltrating $CD8^+$ T cells because ocular tissues express CD95L (FasL) (13), TRAIL (14), and PD-L1/PD-L2 (15), which can induce apoptosis of activated T cells. Similarly, intratumoral accumulation of CTLs could be limited by their exclusion from the established tumor microenvironments after initial migration as was shown in a peritoneal tumor model (16). Another possibility is that CTLs are rendered nonresponsive within the ocular tumor microenvironment, as Ksander et al. (17) demonstrated that T cells within primary uveal melanomas proliferated very poorly after in vitro stimulation. Altered signaling via the TCR may account for this nonresponsiveness, as CD3ζ-chain expression is reduced on T cells in the blood and within tumors of uveal melanoma patients (18, 19). CD3ζ-chain expression may be modulated by $CD11b^+$ myeloid-derived suppressor cells (MDSCs), which expand in the blood and within tumors of patients with certain malignancies (20), including uveal melanoma (18). As increased numbers of macrophages (Mϕs) infiltrating uveal melanomas has been associated with a poor prognosis (21), and as we have shown that $CD11b^+$ cells isolated from ocular tumors in mice inhibit

*Graduate Program in Immunology, [†]Department of Ophthalmology, [‡]Department of Immunology, and [§]Department of Pediatrics, University of Pittsburgh School of Medicine, Pittsburgh, PA 15213; and [¶]Department of Ophthalmology, Emory University, Atlanta, GA 30322

[1]Current address: Department of Cell and Developmental Biology, University of North Carolina at Chapel Hill, Chapel Hill, NC.

Received for publication October 20, 2009. Accepted for publication September 22, 2010.

This work was supported by National Eye Institute Grants R01 EY018355 (to K.C.M.), K23064396 (to T.L.C.), and P30-EY08098, The Eye and Ear Foundation of Pittsburgh, and by an unrestricted grant from Research to Prevent Blindness, Inc.

Address correspondence and reprint requests to Kyle C. McKenna, Department of Ophthalmology, University of Pittsburgh, Eye and Ear Institute, Room 910, 203 Lothrop Street, Pittsburgh, PA 15213. E-mail address: mckennakc@upmc.edu

The online version of this article contains supplemental material.

Abbreviations used in this paper: a.c., anterior chamber; AqH, aqueous humor; ARG1, arginase 1; Gzm B, granzyme B; iMFI, integrated median fluorescence intensity; Mϕ, macrophage; MDSC, myeloid-derived suppressor cell; NMMA, N^G-monomethyl-L-arginine; NOS2, NO synthase; NT, nitrotyrosine; OT-I CTL, OT-I–stimulated splenocyte; SIINFEKL, $OVA_{257–264}$ peptide; SGM, standard growth medium; Treg, regulatory T cell.

Copyright © 2010 by The American Association of Immunologists, Inc. 0022-1767/10/$16.00

Downloaded from http://journals.aai.org/jimmunol/article-pdf/185/11/6706/1325334/0903411.pdf by guest on 20 April 2024

CTL responses in vitro (5), MDSCs could play a role in ocular tumor development by suppressing tumor-specific CTLs. Finally, tumoricidal activity of CTLs could be ineffective because of their failure to induce tumoricidal activity in other cells within the tumor microenvironment that are critical for tumor elimination. For example, Hollenbaugh and Dutton (22) demonstrated that elimination of established skin tumors in mice by CTL transfer therapy required NO production by unidentified host cells, which was induced by IFN-γ expressed by CTLs.

To elucidate the mechanisms of CTL inhibition within the ocular tumor microenvironment, we tracked and functionally characterized tumor-specific CTLs transferred into mice with tumors developing in the a.c. of the eye or in skin. We demonstrate that ocular tumors are resistant to CTL transfer therapy whereas skin tumors are exquisitely sensitive. Transferred CTLs infiltrated both tumor sites and surprisingly displayed similar effector function in terms of cytokine production (TNF, IFN-γ) and granule exocytosis, despite the presence of $CD11b^+$ cells, which were suppressive to CTL responses in vitro via NO production. We extend the previous findings of Hollenbaugh and Dutton (22) by showing that transferred CTLs activate skin tumor-associated $CD11b^+F4/80^+$ Mϕs to produce NO at tumoricidal concentrations. In contrast, ocular tumor-associated myeloid cells, primarily composed of $CD11b^+$ $Gr\text{-}1^+$ cells and few $CD11b^+F4/80^+$ Mϕs in this model, are profoundly inhibited in their tumoricidal capacity because of their inability to produce tumoricidal levels of NO. We conclude that intratumoral myeloid cells do not suppress the effector phase of CTL responses and that the failure of CTLs to control ocular tumor development is due to inhibited tumoricidal activity of intratumoral Mϕs.

Materials and Methods

Experimental animals

Male and female C57BL/6.PL (B6.PL; H-2^b, $CD90.1^+$), C57BL/6 (B6; H-2^b, $CD90.2^+$), B6.129S7-$Rag1^{tm1Mom/J}$ ($RAG1^{-/-}$; H-2^b), B6;129P2-$Nos2^{tm1Lau}$/J ($NOS2^{-/-}$; H-2^b, $CD90.2^+$), BALB/cJ (H-2^d), B6.129S7-$Ifngr1^{tm1Agt}$/J ($IFN\text{-}\gamma R1^{-/-}$, H-$2^b$, $CD90.2^+$), and C57BL/6J-TgN (OT-I; B6; H-2^b, $CD90.2^+$) (23) mice were purchased from The Jackson Laboratory (Bar Harbor, ME). OT-I mice were backcrossed with B6.PL mice to generate $CD90.1^+/CD90.2^+$ and $CD90.1^+$ congenic OT-I mice. All the procedures on animals were approved by the Institutional Animal Care and Use Committee of the University of Pittsburgh (Pittsburgh, PA).

Tumor cell lines

EL-4 cells, EL-4 transduced to express OVA (E.G7-OVA, H-2^b, $CD90.2^+$) (24), and P815 (H-2^d) cells were obtained from American Type Culture Collection (Manassas, VA). Tumor cell lines were grown in standard growth medium (SGM; RPMI 1640 medium supplemented with 10% FBS, 2 mM L-glutamine, 1 mM sodium pyruvate, 50 μM 2-ME, gentamicin, penicillin, and streptomycin) at 37°C in a 5% CO_2 atmosphere and were maintained free of mycoplasma. E.G7-OVA cells were continuously cultured with 1 mg/ml G418 (Invitrogen, Carlsbad, CA) to maintain the expression of the transfected OVA gene then scaled-up in SGM alone in two 3- to 4-d cultures prior to injection.

Tumor cell administration

Tumor cells for injections were recovered at midlog growth phase. A.c. injections (10^4 tumor cells) and intradermal skin injections (10^6 tumor cells) into the right flank were performed as previously described (5).

Tissue processing

Mice were euthanized by asphyxiation with CO_2, and lymph nodes and spleens were removed and rendered into a single-cell suspension by pressing the spleen through a nylon mesh screen (70 μm). RBCs were lysed with Tris-buffered ammonium chloride. After washing with HBSS, cells were resuspended in FACS buffer (PBS plus 1% FBS) or SGM at 2×10^7 cells/ml as determined by cell counts in a Vi-CELL XR counter (Beckman-Coulter, Miami, FL). Tumor-bearing eyes were rendered into a single-cell suspension as previously described (5) and then resuspended in 0.4 ml FACS buffer or SGM. Excised skin tumors were enzymatically digested to obtain single-cell suspensions as described by Zhang et al. (25).

Tumor burden measurements

Skin tumors were measured using a caliper, and the tumor size was calculated by multiplying the measured lengths of two perpendicular axes. The number of E.G7-OVA cells in ocular tumors was determined by flow cytometry as previously described (5) with some modifications. Count Bright absolute counting beads (Invitrogen) were used to collect half of each eye sample from a known initial sample volume (0.1 ml). The number of $CD45^+$ cells within the entire eye was then determined by the following formula: Number of $CD45^+$ cells within collected sample × ([number of beads added/number of beads collected] × 4). Tumor cells were identified as $CD45^+$, $CD90.2^+$, $CD8^-$, and $CD4^{low}$ high forward scatter events. The absolute number of each respective population was then determined by multiplying the number of $CD45^+$ cells in the sample by the percentage of $CD45^+$ cells of each respective cell population.

CTL generation and adoptive transfer

Naive splenocytes from OT-I mice (4×10^6), prepared as described above, were stimulated with 0.1 μg/ml $OVA_{257–264}$ peptide (SIINFEKL) in individual wells of a 24-well plate in a total volume of 2 ml SGM. After incubation for 3 d at 37°C in a 5% CO_2 atmosphere, Ficoll separation was performed to remove dead cells, and the number of live cells was determined by trypan blue exclusion. No further enrichment of the purified activated effector splenocytes was performed because more than 95% of live cells after Ficoll separation were $CD90.2^+$, $CD8^+$, and $OVA_{257–264}$ K^b $tetramer^+$ T cells (Supplemental Fig. 1*A*, 1*B*). OVA-specific lytic activity by OT-I–stimulated splenocytes (OT-I CTLs) was measured in a standard 4-h chromium release assay using $Na_2{}^{51}CrO_4$ (Dupont, Boston, MA) labeled E.G7-OVA and EL-4 targets as previously described (5). Generated OT-I CTLs specifically lysed only targets expressing OVA (Supplemental Fig. 1*C*) and showed high IFN-γ and TNF production, as well as lytic granule release upon in vitro stimulation (Supplemental Fig. 1*D*, 1*E*). For adoptive transfer experiments, OT-I CTLs (3×10^6 cells) were injected i.v. via the tail vein in 200 μl PBS and were tracked in recipient B6 mice in vivo using $OVA_{257–264}$ K^b tetramers or CD90.1 as a congenic marker by flow cytometric analysis (Supplemental Fig. 1*F–I*).

Ocular tumor wholemounts and confocal microscopy

The anterior segment of the eye containing ocular tumors was dissected from the posterior of the eye using surgical scissors. The iris was then removed, and the anterior segment was blocked with purified anti-CD16/32 mAb (BD Pharmingen, San Diego, CA), then incubated with PE-labeled anti-CD90.1, Pacific Blue-labeled anti-CD11b, and FITC-labeled anti-CD90.2 in 100 μl FACS buffer in an individual well of a 96-well plate. Eye tissue was then washed and mounted with Immunomount (ThermoFischer Scientific, Pittsburgh, PA). Confocal microscopy was performed using an Olympus Fluoview 1000× confocal microscope (Olympus, Center Valley, PA), and images were acquired by sequential scanning to prevent fluorescent crossover. All image analysis and reconstructions were performed using Metamorph software (Molecular Devices, Sunnyvale, CA).

Flow cytometry

Eye suspensions (0.1 ml) or 2×10^6 skin tumor cells or splenocytes were added to individual wells of a 96-well plate for staining. Fc receptors were blocked with purified anti-CD16/32 mAb (BD Pharmingen), then cells were incubated with FITC-, PE-, PE-Cy7–, PerCP-, or allophycocyanin-labeled mAbs against CD3ε, CD4, CD8α, CD11c, CD40, CD45, B220 (CD45RB), CD80, CD86, CD90.1, CD90.2, CD107a, CD115 (M-CSF), CD124 (IL-4Rα), F4/80, FcεRI, Gr-1, Ly-6C, Ly-6G, MHC class I (H-$2K^b$/H-2 D^b), NK 1.1 (BD Pharmingen); or Pacific Blue-conjugated CD11b, allophycocyanin-conjugated CD68, AF700-conjugated MHC class II (I-A/I-E) (eBioscience, San Diego, CA), or PE-Cy7–conjugated CD90.2 (Biolegend, San Diego, CA), or allophycocyanin-conjugated H-$2K^b$ tetramers containing the C57BL/6 immunodominant peptide SIINFEKL (Beckman-Coulter, Miami, FL), and fixable violet dead cell stain (Invitrogen). After incubation, wells were washed and resuspended in 0.2 ml FACS buffer or fixed with Cytofix/Cytoperm reagent (BD Pharmingen). When needed, fixation was followed by washes in Perm/Wash buffer (BD Pharmingen). For intracellular staining of OT-I CTLs, cell suspensions were incubated with allophycocyanin-conjugated or PE-Cy7–conjugated anti–IFN-γ, anti-granzyme B, and anti-TNF mAbs (BD Pharmingen) or respective labeled

Downloaded from http://journals.aai.org/jimmunol/article-pdf/185/11/6706/1325334/0903411.pdf by guest on 20 April 2024

isotype control Abs. For intracellular staining of intratumoral myeloid cells, cells were blocked overnight in Perm/Wash buffer (BD Pharmingen) containing 5% donkey serum, then cell suspensions were incubated with unconjugated anti-NO synthase (anti-NOS2) polyclonal rabbit Ab (BD Pharmingen) and mouse anti-arginase 1 (ARG1) mAb (BD Pharmingen), followed by incubation with PE- or AF546-conjugated goat anti-rabbit IgG (Invitrogen) and allophycocyanin-conjugated rat anti-mouse Ig-G1 (BD Pharmingen), respectively. Samples were run on a FACSAria or FACSCalibur flow cytometer (Becton Dickinson, San Jose, CA), and data were analyzed using FACS Diva (Becton Dickinson) and FlowJo software (Tree Star, Ashland, OR). For some experiments, the integrated median fluorescence intensity (iMFI) was calculated by multiplying the percentage of positive cells by the median fluorescence intensity as described elsewhere (26).

Ex vivo stimulation of transferred OT-I CTLs

Tumors and spleens were harvested 6 d after CTL transfer therapy and were rendered into single-cell suspensions as described earlier. Cells (4×10^6) from skin tumor cell suspensions or 0.2-ml ocular tumor cell suspensions were incubated for 6 h at 37°C in a 5% CO_2 atmosphere with or without SIINFEKL peptide (10 μg/ml) in either SGM containing brefeldin A (BD Biosciences) when cytokines were measured or monensin and anti-CD107a mAb (BD Biosciences) when degranulation was measured. After stimulation, cell suspensions were stained to determine surface CD107a expression and intracellular expression of granzyme B, TNF, and IFN-γ by viable OT-I CTLs (violet dead cell stain negative, $CD8^+$, $CD90.2^+$/$CD90.1^+$ cells) using flow cytometry.

Flow cytometric cell sorting of tumor-associated myeloid cells

Skin or eye tumors were rendered into single-cell suspensions, then magnetic cell sorting with the EasySep PE selection kit (Stem Cell Technologies, Vancouver, British Columbia, Canada) was performed to exclude $CD90.2^+$ tumor cells from cell suspensions previous to flow cytometric cell sorting. Nonselected cells were stained with fluorochrome-conjugated anti-CD45, anti-CD11b, and anti–Gr-1 mAbs, and $CD11b^+Gr\text{-}1^+$ and $CD11b^+Gr\text{-}1^-$ cells were then isolated by flow cytometric cell sorting for use in T cell suppression and tumoricidal assays. Purity of sorted populations was always higher than 95% as shown in Supplemental Fig. 2.

T cell suppression assay

Naive splenocytes from OT-I mice were diluted 1:5 with naive splenocytes from B6.Pl mice. Cells (4.0×10^6) were added to an individual well of a 24-well flat-bottom plate with or without the addition of $CD11b^+$ cells (0.5×10^6 cells) isolated from ocular tumors or skin tumors, with or without SIINFEKL (0.1 μg/ml), and with or without the addition of N^G-monomethyl-L-arginine (NMMA; Calbiochem, EMD Biosciences, San Diego, CA) (0.5 mM final concentration) in a total volume of 2 ml SGM. After incubation for 4 d at 37°C in a 5% CO_2 atmosphere, the number of live cells was determined by trypan blue exclusion, and the percentage of live OT-I cells was determined by flow cytometric analysis of cultured cells stained with 7-aminoactinomycin D, FITC-labeled anti-CD8α, and PE-labeled CD90.2. Live OT-I T cells were defined as 7-aminoactinomycin D negative, $CD8\alpha^+$, and $CD90.2^+$. Cultured cells were tested for lytic activity using a standard chromium release assay performed as described earlier.

In vitro tumor growth inhibition assay

E.G7-OVA tumor cells (5×10^3) were cultured with or without 10^5 cells of the indicated flow-sorted $CD11b^+$ cell subset. Three days later, nitrite concentration was determined in culture supernatants using the Griess assay (Promega, Madison, WI), and cells were harvested to determine the percentage of inhibition of E.G7-OVA tumor growth using flow cytometry. Tumor cells were identified as $CD45^+$, $CD90.2^+$, $CD8^-$, $CD11b^-$ high forward scatter events, and Count Bright absolute counting beads (Invitrogen) were used to collect half of each total cell sample to determine the number of tumor cells per sample. Percentage growth inhibition was determined as follows: $100 \times (1 - [\text{number of E.G7-OVA in experimental sample/number of E.G7 in control sample}])$.

Winn-type assays

Mϕs were harvested from the peritoneal cavities of B6 mice that had been injected with 2 ml thioglycolate 4 d previous, and Mϕs were activated in vitro with a combination of IFN-γ (200 U/ml) and TNF (100 U/ml) for 48 h. The activated Mϕs were mixed with E.G7-OVA tumor cells to obtain a 30:1 or 100:1 ratio with a final concentration of 5×10^5 E.G7-OVA/ml, immediately before tumor injection of $RAG1^{-/-}$ mice. Two microliters or 200 μl of these cell suspensions was injected into the a.c. (10^3 tumor cells) or intradermally (10^5 tumor cells) to produce ocular or skin tumors, respectively. Tumor growth was then monitored as described earlier.

Real-time quantitative RT-PCR

RNA was isolated using an RNAeasy kit (Qiagen, Germantown, MD) from whole tumor bearing eyes or skin tumor biopsies. cDNA was then prepared using a high-capacity cDNA reverse transcription kit (Applied Biosystems, Carlsbad, CA), and expression of CXCL1 (primer Mm00433859_m1), CXCL2 (primer Mm00436450_m1), CSF-1 (primer Mm 00432688), CSF-2 (primer Mm 00438328), CSF-3 (primer Mm00438334_m1), and the housekeeping gene PCX (primer Mm00500992_m1) was determined by quantitative real-time PCR using the TaqMan PCR universal mix (Applied Biosystems) and a Step One Plus real-time PCR thermocycler (Applied Biosystems). All primers were obtained from Applied Biosystems. Relative expression was determined by normalizing gene expression (40 − Ct) to the expression of PCX within each sample.

Statistical analysis

Statistical analyses were performed using Prism 5 software (GraphPad, La Jolla, CA). For each studied variable, the mean, median, and SD were calculated, and to determine normality the D'Agostino–Pearson test was used. Differences in indicated cell numbers or percentages were compared by unpaired Student *t* tests or unpaired Mann-Whitney *U* tests depending on the normality of the data. For comparison of multiple groups, one-way ANOVA or Kruskal-Wallis test on ranks with Tukey's or Dunn's multiple comparison post hoc tests to compare the individual groups, respectively, were used depending on the normality of the data. Two-way ANOVA was used for comparison of skin tumor growth over time. Differences in the incidence of measurable tumors were computed with the Kaplan–Meier method, and differences were validated with log-rank test; p values <0.05 were considered statistically significant.

Results

Established ocular tumors are resistant to CTL transfer therapy

E.G7-OVA tumors grow progressively in the a.c. of the eye despite priming for OVA-specific $CD8^+$ T cell responses capable of rejecting a subsequent injection of E.G7-OVA in the skin or opposite eye (5). These data indicate that CTLs can demonstrate effector function within the eye but are inhibited within the established ocular tumor microenvironment. Therefore, to determine the fate of CTLs within ocular tumors, we transferred $CD90.1^+$ OVA-specific OT-I CTL effectors into CD90.2 congenic B6 mice before and 3 or 5 d after injection of E.G7-OVA in the a.c. of the eye.

OT-I CTL transfer before a.c. injection of 10^4 E.G7-OVA delayed the kinetics of ocular tumor growth reducing tumor burden (17-fold) on day 7 in comparison with that in non-transferred control mice (Fig. 1*A*). Over time, however, tumor growth was uncontrolled. Delaying the time of CTL transfer after tumor challenge minimized the effectiveness of CTLs to control ocular tumor growth. For example, when CTLs were transferred 3 d after tumor challenge, tumor burden was reduced by 31-fold on day 11, whereas only a 4-fold reduction was observed when CTL transfer occurred on day 5 (Fig. 1*B*). As in our previous experiment, ocular tumor growth ultimately became uncontrolled. Increasing tumor burden over time could not entirely explain the failure of CTLs to eliminate established ocular tumors because an equivalent CTL transfer before (Fig. 1*C*) or 10 d after (Fig. 1*D*) injection of a much larger tumor challenge (10^6) in the skin mediated rejection of intradermal tumors in the majority of mice, which reproduces previously published observations (22, 27). These data indicated that established ocular tumors were resistant to CTL transfer therapy whereas skin tumors were sensitive.

Tumor-specific CTLs efficiently infiltrate both tumor sites

Failure to control ocular E.G7-OVA tumor growth could be due to limited accumulation of CTLs within ocular tumors or to inhibited

Downloaded from http://journals.aai.org/jimmunol/article-pdf/185/11/6706/1325334/0903411.pdf by guest on 20 April 2024

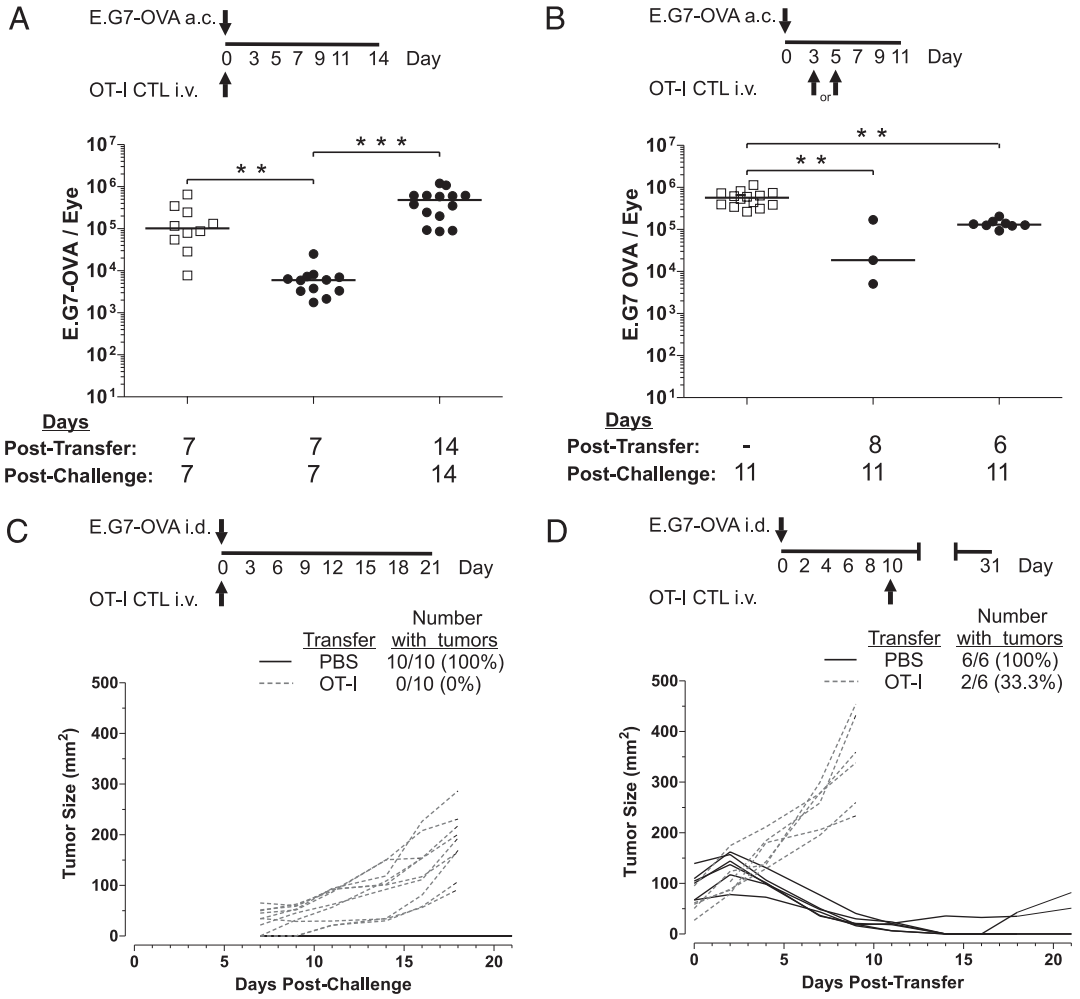

FIGURE 1. Ocular tumors are resistant to tumor-specific CTL transfer therapy. OT-I CTLs were i.v. transferred before (*A*, *C*) or after (*B*, *D*) the injection of E.G7-OVA tumor cells in the a.c. (10^4) (*A*, *B*) or intradermally in the flank (10^6) (*C*, *D*) at the indicated time points. Ocular tumor burden was measured by flow cytometric analysis, and skin tumor measurements were made with a caliper. Each symbol or line indicates the measurement from an individual mouse. For *A* and *B*, lines are medians. The *p* values for *A* were calculated by Kruskal-Wallis test on ranks with Dunn's comparison post test and for *B* by one-way ANOVA and Tukey's multiple comparison post test (data were pooled from at least two independent experiments). $^{**}p < 0.01$; $^{***}p < 0.001$. For *C*, $p < 0.01$ on day 9, and $p < 0.001$ on the subsequent days; for *D*, $p < 0.001$ on days 7 and 9, by two-way ANOVA and Tukey's multiple comparison post test (one experiment shown, representative results from two independent experiments).

CTL migration into the tumor site. Therefore, flow cytometry and confocal microscopy were used to evaluate infiltration of CD90.1$^+$ OT-I CTLs into skin and eye tumors. Five days after injection of E.G7-OVA in the a.c. or 10 d after tumor injection in the skin, mice received an i.v. OT-I CTL transfer. Six days later, flow cytometric analysis was performed and demonstrated that intratumoral CD90.1$^+$ OT-I CTLs were present in both tumor sites and were easily distinguished from CD90.2$^+$ tumor cells and endogenous CD90.2$^+$ T cells (Fig. 2*A*), which were very few in number (Supplemental Fig. 3). Importantly, though ocular tumors were resistant and skin tumors sensitive to CTL transfer therapy, the ratio of OT-I CTLs to tumor cells in ocular tumors was more than 50 times higher than that in skin tumors (Fig. 2*B*). However, our flow cytometric analysis of whole collagenase-digested tumor-bearing eyes did not allow us to discern whether CTLs were present within the ocular tumor or in other areas of the eye. Therefore, confocal microscopy of ocular tumor wholemounts stained with fluorescently labeled Abs was performed. This analysis demonstrated that CD90.1$^+$ OT-I CTLs extensively infiltrated ocular tumors and were in close proximity to CD90.2$^+$ tumor cells and infiltrating CD11b$^+$ myeloid cells (Fig. 2*C*). The migration of tumor-specific CTLs into ocular tumors was regulated by IFN-γ, as IFN-γR1$^{-/-}$ mice demonstrated reduced numbers of infiltrating OT-I CTLs compared with that in wild-type mice (Supplemental Fig. 4). These data indicated that the failure of CTLs to control ocular tumors was not due to impaired infiltration of ocular tumors.

OT-I CTLs demonstrate effector function in the ocular tumor microenvironment

Previous studies have demonstrated that IFN-γ produced by transferred OT-I CTLs is required to promote skin tumor rejection, whereas CTL-expressed perforin, FasL, and TNF are dispensable (22, 27). Therefore, we tested whether differences in IFN-γ production or in other canonical effector functions performed by CTLs infiltrating skin or ocular tumors accounted for the failure of transferred CTLs to control ocular tumor growth. B6 mice were challenged with tumors in the eye (10^4) or skin (10^6). Five days after eye tumor challenge or 10 d after skin tumor challenge, mice received an OT-I CTL transfer. Tumors and spleens from both groups were then harvested and processed independently into single-cell suspensions 6 d after CTL transfer and stimulated ex vivo with SIINFEKL peptide. OT-I CTLs

Downloaded from http://journals.aai.org/jimmunol/article-pdf/185/11/6706/1325334/0903411.pdf by guest on 20 April 2024

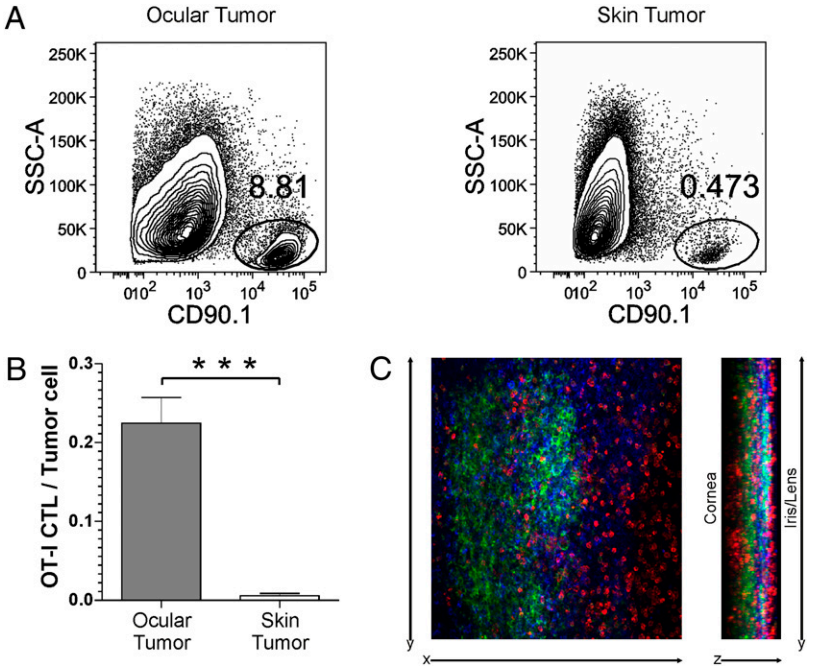

FIGURE 2. CTLs infiltrate ocular tumors and are in close apposition to tumor and myeloid cells. Five or 10 d after injection of 10^4 or 10^6 E.G7-OVA tumor cells in the a.c. or skin, respectively, mice received an i.v. transfer of $CD90.1^+/CD90.2^+$ OT-I CTLs. Six days later, tumors were harvested, and CTL infiltration was examined. *A*, The percentage of transferred $CD90.1^+$ CTLs from a $CD45^+CD90.2^+CD11b^-$ gate present in collagenase-digested skin and ocular tumors was determined by flow cytometric analysis. Numbers indicate the percentage of transferred CTLs. Data for one representative mouse in each group is shown ($n = 4$ per group). *B*, The ratio of OT-I CTLs to tumor cells in skin and ocular tumors from these mice was determined by dividing the number of OT-I CTLs by the number of tumor cells per eye. Bars indicate mean ± SD. Data from one representative experiment are shown of two independent experiments performed. $***p < 0.001$, unpaired two-tailed Student *t* test. *C*, Confocal microscopic images of ocular tumor wholemounts obtained 6 d after OT-I CTL transfer and 11 d after tumor injection. Tissues were stained with Abs against CD90.2 (green), CD90.1 (red), and CD11b (blue) to identify E.G7-OVA cells ($CD90.2^+$, $CD90.1^-$, $CD11b^-$), transferred OT-I CTLs ($CD90.2^-$, $CD90.1^+$, $CD11b^-$), and myeloid cells ($CD90.2^-$, $CD90.1^-$, $CD11b^+$). The *x*- and *y*-axes measure 635.9 μm each, while the *z*-axis measures 95.6 μm. Confocal image shown are from one representative mouse of two independent experiments.

infiltrating both tumor sites exhibited equivalent production of IFN-γ, TNF, and granzyme B and comparable release of lytic granules, as measured by CD107a expression (Fig. 3). Notably, tumor-infiltrating OT-I CTL expression of both IFN-γ and TNF was markedly reduced compared with that of splenic CTLs at both tumor sites (Fig. 3). These data indicated that canonical CTL effector functions were not compromised within the ocular tumor microenvironment.

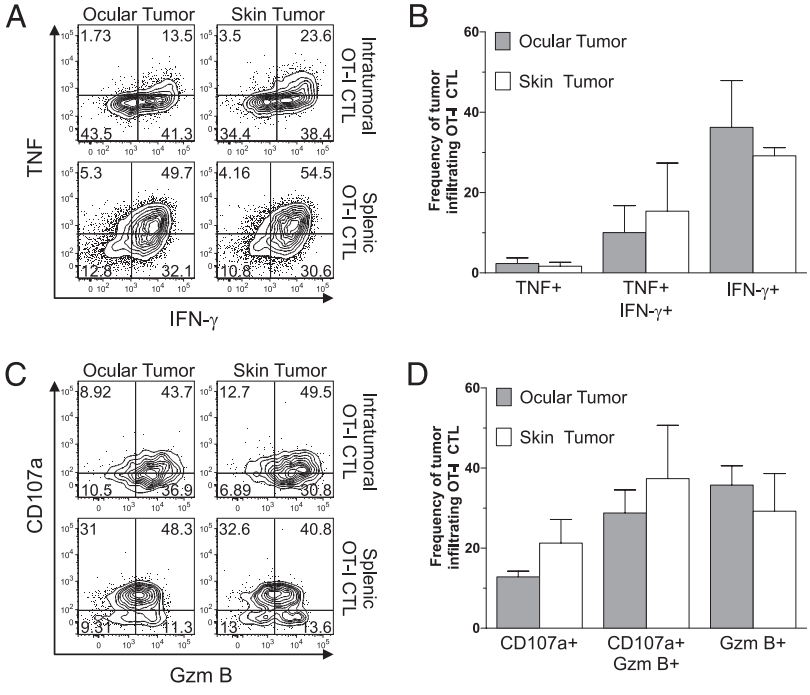

FIGURE 3. Tumor-infiltrating OT-I CTLs exhibit similar effector function in skin and ocular tumor microenvironments. Cytokine production and granule exocytosis by tumor-infiltrating $CD90.1^+$ OT-I CTLs was determined by flow cytometric analysis. Contour plots display expression of IFN-γ and TNF (*A*) or granzyme B (Gzm B) and CD107a (*C*) by gated transferred OT-I CTLs, respectively. Data shown are from a representative mouse of each group ($n = 4$ per group); numbers indicate the percentage of cells within each quadrant. Mean percentages of OT-I CTLs positive only for one marker or for both from all mice within each group ($n = 12$ per group) are shown in *B* and *D*. Data shown were pooled from three independent experiments; scale bars indicate mean ± SD.

Downloaded from http://journals.aai.org/jimmunol/article-pdf/185/11/6706/1325334/0903411.pdf by guest on 20 April 2024

Characterization of intratumoral myeloid cell populations in skin and ocular tumors

We previously demonstrated that ocular tumors were heavily infiltrated by $CD11b^+Gr\text{-}1^+$ cells and that $CD11b^+$ cells isolated from ocular tumors inhibited CTL activity in vitro (5). Therefore, we characterized the $CD45^+$ infiltrate of both skin and eye tumors by flow cytometry to determine whether differences in myeloid cell subsets may be associated with sensitivity or resistance to CTL transfer therapy. Greater than 95% of $CD45^+$ cells within ocular and skin tumors of C57BL/6 mice were composed of $CD90.2^+$ cells and $CD11b^+$ cells (Fig. 4*A*). In non-CTL-transferred mice, 99% of these $CD90.2^+$ cells within ocular tumors were E.G7-OVA tumor cells and the remainder was endogenous tumor-infiltrating $CD3\varepsilon^+$ cells as shown by the characterization of the cellularity of ocular tumors in CD90.1 congenic B6.PL mice and $RAG1^{-/-}$ mice (Supplemental Fig. 3). This characterization of ocular tumors also indicated that the small percentage of $CD45^+$ cells (~3–5%) that were not tumors or $CD11b^+$ cells were primarily $CD4^-CD8^-CD3\varepsilon^+$ T cells, $B220^+$ cells, and NK 1.1^+ cells (Supplemental Fig. 3*B*). $Fc\varepsilon RI^+$ mast cells were not observed (Supplemental Fig. 3*B*). The number of tumors was comparable in B6.PL and RAG-$1^{-/-}$ mice, whereas a modest (2-fold) reduction was observed in CD11b numbers in $RAG1^{-/-}$ mice indicating that T cells were largely not required for $CD11b^+$ cell infiltration (Supplemental Fig. 3).

Ocular tumors were composed of a greater percentage of $CD11b^+$ cells in comparison with skin tumors (Fig. 4*A*). The proportion of tumor cells to $CD11b^+$ cells in ocular and skin tumors that received a CTL transfer or were untreated did not differ significantly at the examined time point (Fig. 4*A*, 4*B*). However, striking differences in the composition of intratumoral $CD11b^+$ myeloid cell subsets were observed, as $CD11b^+Gr\text{-}1^+F4/80^-$ cells predominated in ocular tumors (63.81 ± 9.6% of $CD11b^+$ events), reproducing our previous results (5), whereas $CD11b^+Gr\text{-}1^-F4/80^+$ cells predominated in skin tumors (76.48 ± 4.1% of $CD11b^+$ events) (Fig. 4*C*, 4*D*). Upon OT-I CTL transfer therapy of day 5 ocular E.G7-OVA tumors, the percentage of intratumoral $CD11b^+Gr\text{-}1^-F4/80^+$ Mϕs doubled, whereas within E.G7-OVA skin tumors of CTL transferred mice, the percentage was unchanged (Fig. 4*C*, 4*D*). These data indicated that increased percentages of intratumoral $F4/80^+$ cells were associated with tumor regression.

The percentage of $CD11b^+Gr\text{-}1^+$ cells within ocular tumors of B6.PL mice and $RAG1^{-/-}$ mice was equivalent indicating that T cells were not required for $Gr\text{-}1^+$ cell accumulation though T cells partially contributed to $F4/80^+$ cell infiltration (Supplemental Fig. 3). The unique accumulation of $Gr\text{-}1^+$ cells within ocular tumors may have been due to differences in the expression of chemokines that induce their recruitment, as a 3-fold increase in CXCL2 expression was observed within ocular tumors (Supplemental Fig. 5*A*). However, $Gr\text{-}1^+$ cell accumulation was not common to all tumors developing in the eye, as P815 tumors injected into the a.c. of BALB/cJ mice were infiltrated primarily by $CD11b^+Gr\text{-}1^-F4/80^+$ Mϕs (Supplemental Fig. 5*B*).

Further characterization of the phenotype of $Gr\text{-}1^+$ and $Gr\text{-}1^-$ myeloid cell subpopulations was also performed (Supplemental Fig. 6). These myeloid cell subpopulations differed in their expression of Ly-6G and Ly-6C, with $Gr\text{-}1^-$ cells being completely negative for Ly-6G but partially positive for Ly-6C, whereas $Gr\text{-}1^+$ cells expressed high levels of both markers (Supplemental Fig. 6*A*). In addition, $Gr\text{-}1^-$ cells expressed high levels of F4/80 and CD68 in both tumor sites, whereas $Gr\text{-}1^+$ cells expressed lower levels of these markers. A greater percentage of $Gr\text{-}1^-$ cells expressed CD11c, whereas comparable expression of CD124 and CD115 was observed between $Gr\text{-}1^+$ and $Gr\text{-}1^-$ cells in ocular tumors. CD115 expression was greater in $Gr\text{-}1^-$ cells than in $Gr\text{-}1^+$ cells of skin tumors (Supplemental Fig. 6*A*). These data indicated that $Gr\text{-}1^-$ cells were essentially composed of Mϕ. This

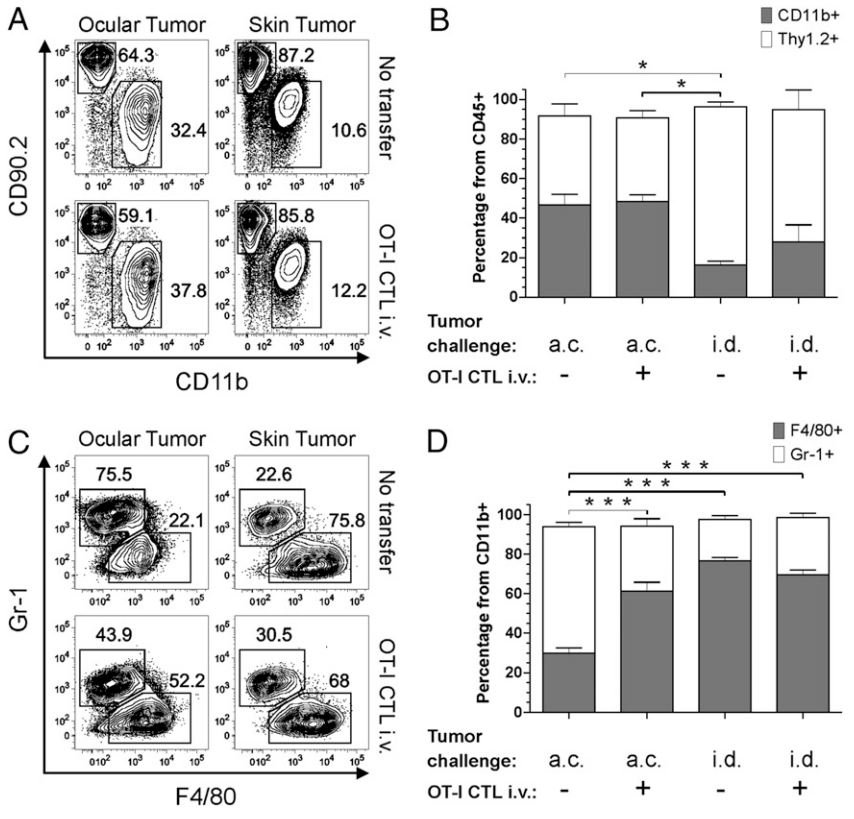

FIGURE 4. Characterization of intratumoral myeloid cells. *A*, Five days or 10 d after injection of E.G7-OVA tumor cells in the a.c. or intradermally, respectively, mice received an i.v. transfer of $CD90.1^+$ OT-I CTLs or were left untreated. Six days later, tumors were rendered into single-cell suspensions, and flow cytometry was performed to determine the percentage of $CD90.2^+$ tumors and $CD11b^+$ cells. Contour plots display results from one representative mouse of four per group; numbers indicate the percentage of cells within each quadrant. *B*, Percentages from all mice within each group. Data shown were pooled from six independent experiments; bars indicate mean ± SD. $*p < 0.05$, one-way ANOVA and Tukey's multiple comparison post test for both percentages of $CD90.2^+$ and $CD11b^+$ cells. *C*, Gr-1 and F4/80 expression of gated $CD45^+CD11b^+CD90.2^-$ cells. Contour plots are from one mouse that is representative of each group; numbers indicate the percentage of cells within each quadrant. *D*, Mean percentages of $Gr\text{-}1^+F4/80^-$ and $Gr\text{-}1^-F4/80^+$ cells from total $CD11b^+$ cells of all mice within each group. Data shown were pooled from six independent experiments; bars indicate mean ± SD. $***p < 0.001$, one-way ANOVA and Tukey's multiple comparison post test for both percentages of $Gr\text{-}1^+$ and $F4/80^+$ cells.

Downloaded from http://journals.aai.org/jimmunol/article-pdf/185/11/6706/1325334/0903411.pdf by guest on 20 April 2024

conclusion was further supported by the almost exclusive expression of high levels of MHC class I, MHC class II, and costimulatory molecules (CD40, CD80, CD86) in the Gr-1$^-$ subpopulation (Supplemental Fig. 6*B*). CD40 expression was reduced in ocular tumor-associated Mϕs, which is consistent with other published observations (28). Notably, the levels of MHC class I, MHC class II, and CD86 appear to be regulated by IFN-γ as these molecules were downregulated in IFN-γR1$^{-/-}$ mice whereas the levels of CD40 and CD80 were essentially IFN-γ independent in our model system (Supplemental Fig. 6*B*).

Immunosuppressive and tumoricidal activities of intratumoral CD11b$^+$ cells are mediated by NO

To determine whether myeloid cells isolated from eye but not skin tumors were suppressive to T cell responses, OT-I T cells were stimulated with cognate Ag in the presence of CD11b$^+$ cells isolated from eye (Fig. 5*A–C*) and skin tumors (Fig. 5*D*–F) of non–CTL-transferred mice. Myeloid cells isolated from both tumor sites suppressed the lytic activity of CTLs primarily by inhibiting CTL expansion. This suppression by tumor-associated CD11b$^+$ cells was mediated by NO, as nitrite levels, an indirect measure of NO production, were elevated in supernatants of cultures containing tumor-associated CD11b$^+$ cells, and the addition of NMMA, an inhibitory L-arginine analogue, inhibited NO production and restored lytic activity.

Paradoxically, Hollenbaugh and Dutton (22) demonstrated that the regression of established E.G7-OVA skin tumors by transferred OT-I CTLs required IFN-γ expression by CTLs and IFN-γR expression and NO production by host cells. As CD11b$^+$F4/80$^+$ Mϕs produce tumoricidal NO when stimulated with IFN-γ and TNF, we hypothesized that interactions between CTLs and intratumoral F4/80$^+$ Mϕs to induce tumoricidal concentrations of NO were critical for skin tumor elimination and that reduced production of NO by F4/80$^+$ Mϕs within the ocular tumor microenvironment could explain CTL evasion by ocular tumors.

To determine the tumoricidal activity of intratumoral myeloid cell populations from both tumor sites, flow cytometric cell sorting was used to isolate CD11b$^+$Gr-1$^+$ and CD11b$^+$Gr-1$^-$ populations (Supplemental Fig. 2), the latter being primarily composed of F4/80$^+$ cells as shown in Fig. 4*C*. In vitro tumor growth was markedly inhibited by F4/80$^+$ Mϕs (96% inhibition) and to a lesser extent by Gr-1$^+$ myeloid cells (44% inhibition) isolated from skin tumors of CTL transferred mice but not by myeloid cells isolated from non-transferred mice (Fig. 6*A*). In contrast, F4/80$^+$ Mϕs and Gr-1$^+$ myeloid cells isolated from ocular tumors of CTL transferred mice failed to inhibit in vitro tumor growth (Fig. 6*A*). Tumor growth inhibition by skin tumor-associated F4/80$^+$ Mϕs was associated with increased nitrite in culture supernatants (Fig. 6*A*). To evaluate NO production in vivo, nitrotyrosine (NT) levels were measured in skin and ocular tumors of B6 mice, IFN-γR1$^{-/-}$ mice, and NOS2$^{-/-}$ mice (negative control). CTL transfer increased NT levels in skin but not eye tumors, which showed NT levels equivalent to tumors in NOS2$^{-/-}$ mice. These data confirm in vivo production of NO within skin but not ocular tumor microenvironments (Fig. 6*B*). NT levels were reduced in skin tumors of CTL transferred IFN-γR1$^{-/-}$ mice indicating the contribution of IFN-γ toward inducing NO production by intratumoral Mϕs. Furthermore, skin tumor regression was not observed in CTL transferred NOS2$^{-/-}$ mice (Fig. 6*C*), reproducing previously published results (22), and the transient regression of ocular tumors upon CTL transfer was unchanged in NOS2$^{-/-}$ mice (Fig. 6*D*). These data indicate that direct CTL activity remains in NOS2$^{-/-}$ mice and is responsible for only a temporary reduction in ocular or skin tumor burden. Compromised tumoricidal activity in intratumoral Mϕs thereby results in progressive tumor growth.

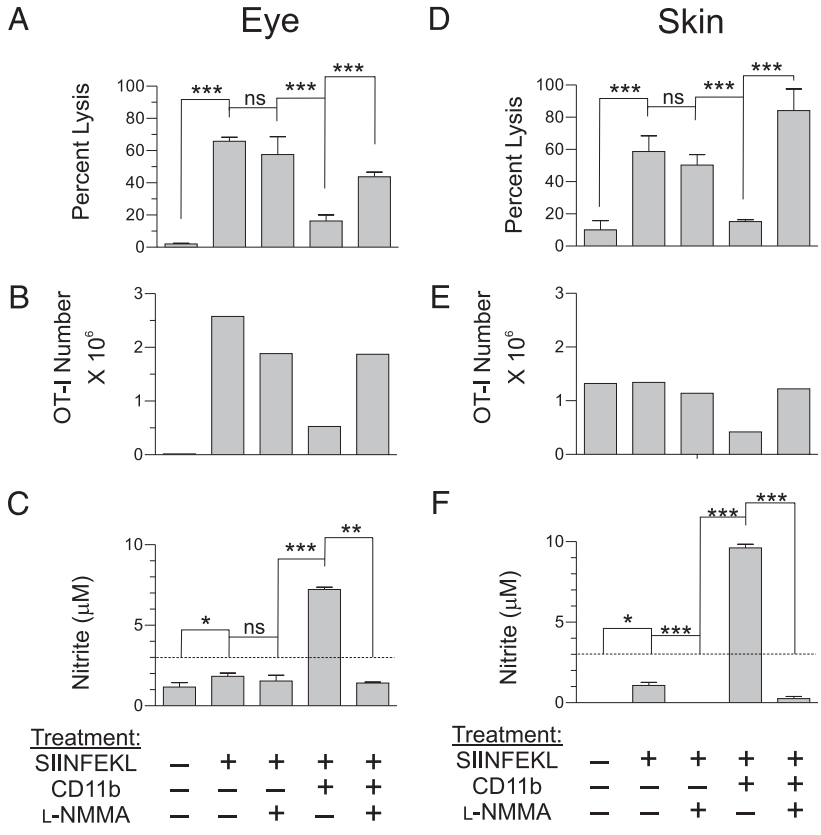

FIGURE 5. Tumor-associated CD11b$^+$ cells inhibit T cell proliferation by NO production. Splenocytes from OT-I mice were untreated or stimulated with cognate Ag (SIINFEKL) in the presence or absence of tumor-associated CD11b$^+$ cells isolated from the eye (*A–C*) or skin (*D–F*), and with and without L-NMMA, an inhibitor of NOS2 activity. After 4 d of incubation, lytic activity against chromium-labeled E.G7-OVA cells was measured at a 67:1 effector/target ratio (*A*, *D*), the number of OT-I T cells within each culture was quantified by flow cytometry (*B*, *E*), and nitrite concentrations in culture supernatants were measured using the Griess assay (*C*, *F*). *A–C* and *D–F* display results from a single experiment that is representative of four independent experiments for ocular tumor-associated myeloid cells and two independent experiments for skin tumor-associated myeloid cells. Nitrite was measured in one experiment for ocular tumor-associated myeloid cells and in both experiments for skin tumor-associated myeloid cells. Dashed line in *C* and *F* indicates the threshold of detection for the measurement of nitrite by the Griess assay. $*p < 0.5$; $**p < 0.01$, $***p < 0.001$, one-way ANOVA and Tukey's multiple comparison post-test.

Downloaded from http://journals.aai.org/jimmunol/article-pdf/185/11/6706/1325334/0903411.pdf by guest on 20 April 2024

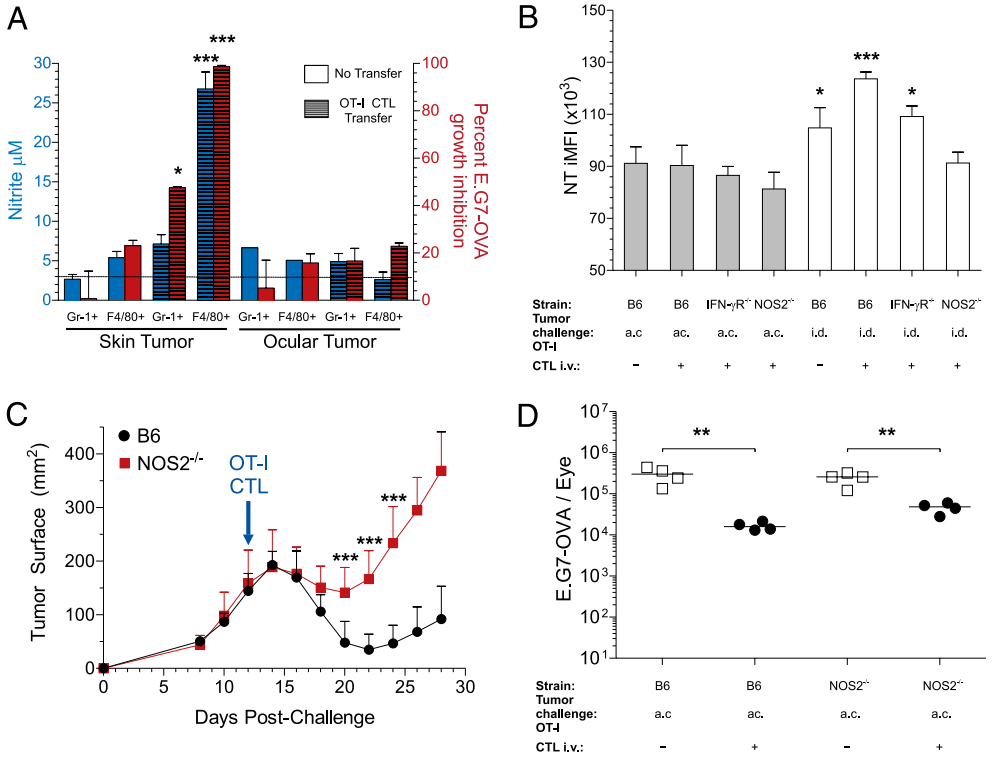

FIGURE 6. Ocular tumors are infiltrated by F4/80$^+$ Mϕs that display impaired NO-dependent tumoricidal activity. *A*, Sorted CD11b$^+$Gr-1$^+$ and CD11b$^+$ Gr-1$^-$ cells from skin and ocular tumors of control and CTL transferred mice were cocultured with E.G7-OVA tumor cells in vitro, and the percentage of E.G7-OVA tumor growth inhibition (red bars) and the concentration of nitrite (blue bars) produced by the different myeloid cell populations were determined. Data shown are representative results pooled from two independent experiments. Dashed line indicates the threshold of detection for the measurement of nitrite by the Griess assay. *$p < 0.05$; ***$p < 0.001$, comparison with all groups by two-way ANOVA and Tukey's multiple comparison post test. *B*, Nitrotyrosine levels within skin and ocular tumors of CTL transferred or non-transferred B6, NOS2$^{-/-}$, or IFN-γR1$^{-/-}$ mice were measured by flow cytometric analysis. Data are presented as iMFIs of NT$^+$ tumor cells. Results from one experiment of two experiments performed demonstrating similar results are shown. *$p < 0.05$; ***$p < 0.001$, comparison with all groups by two-way ANOVA and Tukey's multiple comparison post test. *C*, E.G7-OVA tumor cells (10^6) were injected intradermally in the skin of wild-type B6 mice (black lines) and NOS2$^{-/-}$mice (red lines). Thirteen days later, both groups of mice received an OT-I CTL transfer (blue arrow). Tumor growth was monitored on indicated days by caliper measurements. Each point represents mean ± SD. Data shown represent results from one of three independent experiments performed. ***$p < 0.001$, two-way ANOVA and Tukey's multiple comparison post test. *D*, E.G7-OVA cells (10^4) were injected into the a.c. of the B6 and NOS2$^{-/-}$ mice. Five days later, all mice received an OT-I CTL transfer, and tumor burden was measured 6 d after transfer using flow cytometric analysis. Each symbol indicates the measurement from an individual mouse; lines are medians. Data shown represent results from one of two independent experiments. **$p < 0.01$, one-way ANOVA and Tukey's multiple comparison post test.

Inhibited NO production within ocular tumor-associated Mϕs is not associated with decreased NOS2 protein expression

To identify potential mechanisms responsible for decreased NO production in ocular tumor-associated myeloid cells, the expression of NOS2 and ARG1 proteins in ocular or skin tumor-associated CD11b$^+$ cells was evaluated by flow cytometric analysis (Fig. 7). Gr-1$^+$ myeloid cells within both tumor microenvironments were primarily negative for NOS2 and ARG1 regardless of whether mice received a CTL transfer (Fig. 7*A*). In contrast, the majority of ocular and skin tumor-associated F4/80$^+$ Mϕs expressed ARG1 but only low levels of NOS2 in non-transferred mice. Upon CTL transfer, ARG1 expression was maintained, but the expression of NOS2 increased 10-fold in both skin and eye tumors (Fig. 7*A*, 7*B*) indicating that inhibited NO production by ocular tumor-associated Mϕs was not due to decreased NOS2 protein expression. CTL transfer of IFN-γR1$^{-/-}$ mice did not increase NOS2 expression within ocular tumor-associated Mϕs indicating that induction of NOS2 protein in intratumoral Mϕ cells by CTL transfer was IFN-γ dependent. These data also confirmed that IFN-γ expression by infiltrating CTLs was not compromised within the eye and indicated that Mϕs integrated signals provided by infiltrating CTLs. NOS2 was expressed exclusively by intratumoral myeloid cells and, notably, by E.G7-OVA tumors (Supplemental Fig. 7) confirming the observations of Hu et al. (29).

Tumoricidal activity of activated F4/80$^+$ Mϕs is inhibited within the eye

Numerous molecules, including TGF-β_2, α-melanocyte-stimulating hormone, and calcitonin gene-related peptide, present in normal aqueous humor (AqH), the fluid filling the a.c., are capable of suppressing various aspects of Mϕ activation (30). To explore the possibility that the normal a.c. microenvironment was capable of suppressing activated Mϕs, we tested whether in vitro activated Mϕs displaying tumoricidal activity could be inactivated in vivo by placement into the a.c. of the eye using Winn-type assays (31). Thioglycolate-elicited F4/80$^+$ Mϕs were harvested from the peritoneal cavities of B6 mice and then activated in vitro to induce tumoricidal activity. Activated F4/80$^+$ Mϕs were then mixed with E.G7-OVA cells immediately before a.c. or intradermal injection of RAG1$^{-/-}$ mice. RAG1$^{-/-}$ mice were used in these experiments to remove the contribution of endogenous tumor-specific CD8$^+$ T cell responses, which inhibit the development of skin tumors when mice are injected with limited numbers of tumor cells intradermally (5).

Downloaded from http://journals.aai.org/jimmunol/article-pdf/185/11/6706/1325334/0903411.pdf by guest on 20 April 2024

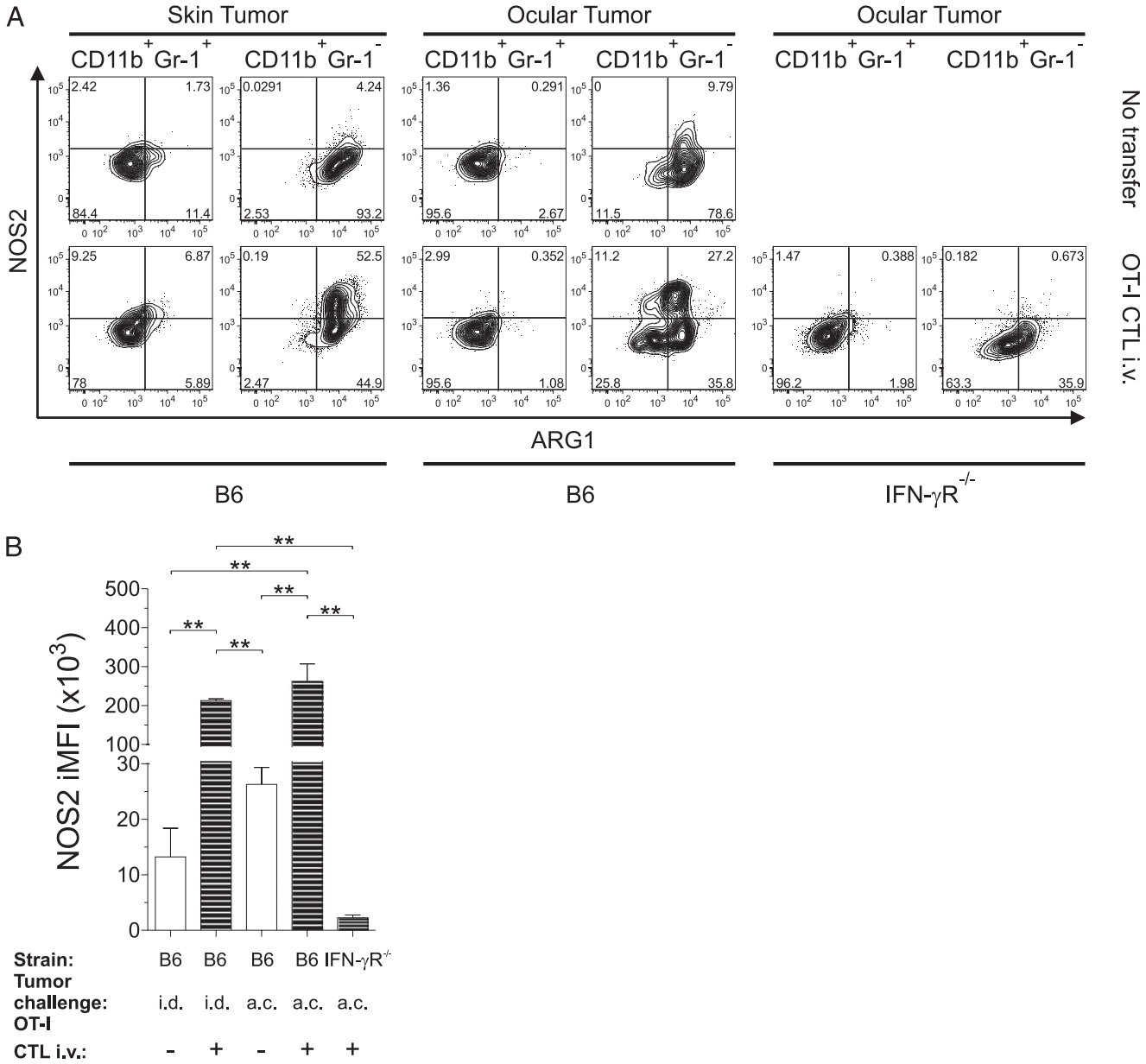

FIGURE 7. NOS2 and ARG1 expression within skin and ocular tumor-associated myeloid cells. B6 and IFN-γR1$^{-/-}$ mice were injected with E.G7-OVA tumor cells in the skin or a.c. Ten days after skin tumor challenge or 5 d after eye tumor injection, mice were untreated or received OT-I CTL i.v. Four days later, cell suspensions of skin tumors and whole tumor-bearing eyes were prepared, and the expression of NOS2 and ARG1 was evaluated using intracellular staining and flow cytometric analysis. *A*, Contour plots show NOS2 and ARG1 expression by intratumoral CD11b$^+$Gr1$^+$ and CD11b$^+$Gr-1$^-$ myeloid cells from control and CTL transferred mice. Data shown are from a representative mouse of each group ($n = 4$), and numbers indicate the percentage of cells within each quadrant. *B*, iMFIs of all NOS2$^+$ Mϕs are shown. This gate includes NOS2$^+$ARG1$^-$ and NOS2$^+$ARG1$^+$ Mϕs. Data shown are from one experiment representative of four independent experiments; bars indicate mean ± SD. $^{**}p < 0.01$, two-way ANOVA and Tukey's multiple comparison post test.

The a.c. microenvironment suppressed the tumoricidal activity of activated F4/80$^+$ Mϕs as evidenced by equivalent ocular tumor numbers in mice injected with tumors alone or with tumors and activated F4/80$^+$ Mϕs (Fig. 8*A*). In contrast, activated F4/80$^+$ Mϕs reduced the initial tumor burden in the skin delaying the kinetics of skin tumor growth (Fig. 8*B*) and reducing the incidence of measurable skin tumors (Fig. 8*C*). OT-I CTLs co-injected with E.G7-OVA cells into the a.c. transiently reduced the number of tumor cells in the eye, confirming that CTL activity was not inhibited in the eye (Supplemental Fig. 8). Therefore, the ocular microenvironment alone is capable of completely suppressing the effector function of activated F4/80$^+$ Mϕs but not that of CTLs.

Discussion

The mechanisms that inhibit tumoricidal activity of CTLs within an ocular tumor microenvironment are not fully understood. Miki et al. (32) demonstrated that tumor-specific CTLs injected intratumorally completely eliminated ocular tumors in mice when the CTL/tumor cell ratio was 1:6, whereas a ratio of 1:50 failed to cure. Therefore, one proposed explanation is that primary ocular tumor growth outpaces priming and expansion of CTLs in secondary lymphoid organs. Hence, primed CTL effectors infiltrating primary ocular tumors could encounter an unmanageable number of tumor cells. However, our data indicate that this simplistic explanation cannot explain the failure of CTLs to control ocular

Downloaded from http://journals.aai.org/jimmunol/article-pdf/185/11/6706/1325334/0903411.pdf by guest on 20 April 2024

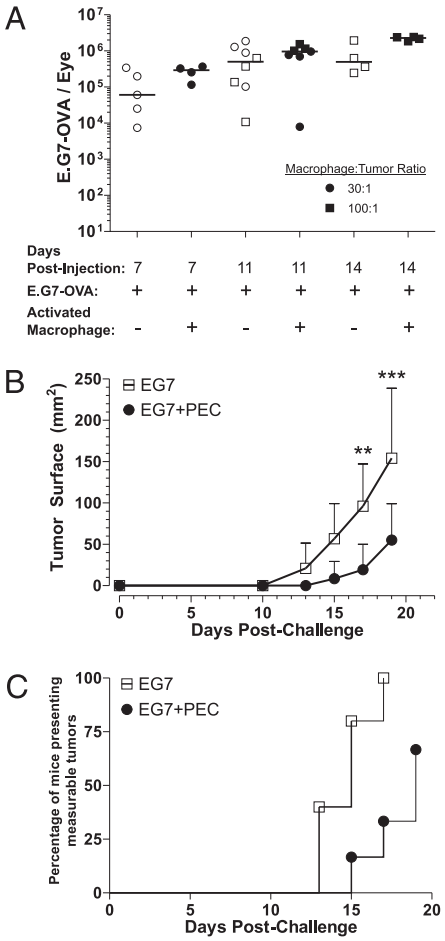

FIGURE 8. The ocular microenvironment suppresses the tumoricidal activity of Mϕs activated in vitro. *A*, Thioglycolate-elicited peritoneal Mϕs were harvested from the peritoneal cavities of B6 mice, activated in vitro, recovered, mixed with E.G7-OVA tumor cells to obtain a 30:1 and 100:1 Mϕ to tumor cell ratio, and then injected into the a.c. of RAG1$^{-/-}$ mice. RAG1$^{-/-}$ mice that received the same number of tumor cells alone were used as controls. Data are representative of results from two independent experiments. Lines displayed are medians. *B*, Cellular suspensions at a 100:1 Mϕ to tumor cell ratio were injected into the skin of RAG1$^{-/-}$ mice. Control mice received the same number of tumor cells alone. Tumor growth was then monitored by caliper measurements. Each point represents mean ± SD. $^{**}p < 0.01$; $^{***}p < 0.001$, two-way ANOVA and Tukey's multiple comparison post test. *C*, The incidence of measurable tumors in these mice was also determined. Data shown represent results from one of two independent experiments. $p = 0.0135$, log-rank test.

tumors because a CTL transfer that is unable to control ocular tumor growth eliminates a much larger tumor burden (100-fold) in the skin (Fig. 1).

CTLs were not excluded from ocular tumors, rather, the CTL/tumor cell ratio was greater in ocular tumors than in skin tumors (Fig. 2). This result was intriguing because the tissues lining the a.c. of the eye express CD95L (FasL) (13), TRAIL (14), and PD-L1/PD-L2 (15), which are capable of inducing apoptosis of activated CTLs that express CD95 (Fas), TRAIL-R2 (DR5), and PD-1. However, our studies cannot exclude the possibility that ocular tumor growth decreased expression of these death-inducing molecules on ocular tissues allowing CTLs to accumulate within ocular tumors. Regardless, CTLs infiltrating ocular tumors were ineffective at controlling progressive tumor growth, and lower CTL/tumor ratios promoted rejection of skin tumors in the majority of mice.

We anticipated that CTLs infiltrating ocular tumors would be functionally inhibited within the eye because PD-L1, a molecule that can induce CTL exhaustion (33, 34), is expressed in the a.c. Moreover, normal AqH contains immunosuppressive molecules including TGF-β2, vasoactive intestinal peptide, somatostatin, and α-melanocyte-stimulating hormone, which can inhibit T cell effector function and/or promote conversion to FoxP3$^+$ T regulatory cells (Tregs) (30). However, we observed no differences in cytokine production or granule exocytosis between PD-1$^+$ CTLs (data not shown) infiltrating tumors developing in the skin and those infiltrating tumors developing in the eye (Fig. 3). One explanation for these results is that CTL effectors that were generated in vitro were less susceptible to immunosuppressive molecules expressed within the eye. However, endogenous CD8$^+$ T cells primed by ocular tumor growth in one eye were shown to differentiate into CTL effectors that rejected a subsequent challenge with the original tumor in the opposite eye (5, 8). These data indicate that endogenous CTL effectors generated by ocular tumor growth in vivo are also functional within the eye. In addition, UV5C25, an ultraviolet-induced fibrosarcoma, is spontaneously rejected by tumor-specific CD8$^+$ T cells in the eye (35) providing further support that CTL effector function is not compromised within the a.c. of normal or tumor-bearing eyes. Therefore, our data clearly indicate that in vitro-differentiated CTLs are not inhibited in the ocular tumor microenvironment, suggesting another critical effector cell being dysfunctional.

Hollenbaugh et al. (27) showed that direct lysis of E.G7-OVA tumor cells by CTLs is not required to promote skin tumor rejection, as transferred CTLs deficient in perforin, TNF, or FasL eliminated established skin tumors. CTL expression of IFN-γ, however, was critical for tumor regression and acted indirectly by induction of NOS2-mediated tumoricidal activity in another cell population, as IFN-γ alone or in combination with TNF did not affect E.G7-OVA growth in vitro, and CTL transfer failed to eliminate E.G7-OVA skin tumors in IFNγR1$^{-/-}$ and NOS2$^{-/-}$ mice (22). We have reproduced and extended these observations by identifying intratumoral CD11b$^+$F4/80$^+$ Mϕs as the critical NO-producing tumoricidal effectors induced by transferred CTLs (Fig. 6*A* and Supplemental Fig. 7). Most importantly, we demonstrate that ocular tumor-associated Mϕs fail to produce tumoricidal concentrations of NO despite NOS2 protein expression, which is induced by IFN-γ expressed by tumor-infiltrating CTLs (Fig. 7). These data suggested that NOS2 enzymatic activity was compromised within the ocular tumor microenvironment, which was supported by the observation that NO-mediated tumoricidal activity was inhibited when activated NOS2$^+$ Mϕs were injected in the a.c. (Fig. 8*A*). Therefore, immunosuppressive mechanisms within the eye that inhibit tumoricidal activity of Mϕs by inhibiting NO production contribute to the failure to control ocular tumors by CTLs.

Taylor et al. (36) showed that Mϕs stimulated in the presence of AqH failed to produce NO despite expression of NOS2, which supports our observations that the ocular microenvironment is suppressive to Mϕ function via posttranslational regulation of NOS2. Posttranslational regulation of NOS2 could be mediated by limiting L-arginine entry into the cell through modulation of the cationic amino acid transporter 2b (37), by limiting production of the cofactor tetrahydrobiopterin by guanosine triphosphate cyclohydrolase 1 (38), or by a competition for limited L-arginine by ARG1 or ARG2, which have V_{max}/K_m values similar to those of NOS2 (39). Our data indicate that competition for L-arginine between NOS2 and ARG1 does not explain limited NO production by ocular tumor-associated Mϕs because our assays to evaluate tumoricidal or immunosuppressive activity of myeloid

Downloaded from http://journals.aai.org/jimmunol/article-pdf/185/11/6706/1325334/0903411.pdf by guest on 20 April 2024

cells were performed in RPMI 1640 medium, which contains a high concentration of L-arginine (1.15 mM) capable of overcoming substrate competition between NOS2 and ARG1 or ARG2 (40). Therefore, future experimentation will focus on cofactor availability and regulatory proteins as they relate to regulation of homodimerization of NOS2, which is a requirement for its activity (41).

We observed a dramatic difference in $CD11b^+$ myeloid cell subsets within skin and ocular tumors suggesting that factors that are unique to each tumor microenvironment shape components of the tumor stroma. We do not fully understand why $Gr\text{-}1^+$ myeloid cells accumulated to such a greater extent in ocular tumors. However, $CD11b^+$ subsets were equivalent in ocular tumors developing within immunodeficient $RAG1^{-/-}$ mice indicating that tumor-derived factors and not infiltrating T cells dictated myeloid cell accumulation in the eye. In addition, we demonstrated that CXCL2, which is chemotactic for $Gr\text{-}1^+$ cells, was increased in ocular tumors, which could suggest a possible mechanism for the accumulation of $Gr\text{-}1^+$ cells in ocular E.G7-OVA tumors. Eye-derived $F4/80^+$ Mϕs have been shown to express CXCL2, which is critical for the recruitment of NKT cells to the spleen that contribute to the generation of systemic tolerance to ocular Ags (42). Therefore, these data could suggest that the ocular microenvironment may selectively upregulate CXCL2 in activated Mϕs, which results in $Gr\text{-}1^+$ cell accumulation. However, pronounced Gr-1 accumulation was not observed when a different tumor cell line, P815, was injected into the a.c. indicating that Gr-1 accumulation was specific to E.G7-OVA tumors and not the ocular microenvironment (Supplemental Fig. 5*B*). The unique factors that regulate chemokine expression within ocular E.G7-OVA tumors will require further experimentation, and our data cannot exclude that differences in the differentiation of $Gr\text{-}1^+$ cells into $F4/80^+$ Mϕs within the tumor microenvironment, which has been demonstrated in EL-4 skin tumors (43), may also be involved.

We previously demonstrated that $CD11b^+$ cells isolated from ocular tumors suppressed the generation of CTLs in in vitro cocultures (5) suggesting that these cells might be MDSCs that could promote ocular tumor growth by inhibiting CTL responses. In this study, we have reproduced and extended that observation by identifying NO as the mediator of this suppression. Notably, as shown in Fig. 7, the cell type that produces NO within nontransferred tumors was exclusively $CD11b^+Gr\text{-}1^-F4/80^+$ Mϕ, suggesting that these cells were solely responsible for inhibiting T cell proliferation in T cell/intratumoral $CD11b^+$ cell cocultures. These results are consistent with observations made by other researchers that indicate that intratumoral $CD11b^+Gr\text{-}1^-F4/80^+$ Mϕs (43) or splenic $CD11b^+Gr\text{-}1^{low}F4/80^+$ Mϕ-like cells (44) are the main cell type responsible for T cell suppression in these in vitro coculture assays. Moreover, we showed that the concentration of NO necessary to inhibit T cell responses in vitro was much lower than the concentration required for tumoricidal activity, highlighting the different roles NO can play in the interactions between tumors and the immune system depending on its local concentration. However, despite demonstrating clear suppressive activity of $CD11b^+$ myeloid cells isolated from skin and ocular tumors toward T cells in vitro, CTL effector function was preserved in both tumor sites in vivo, and in the case of CTL transferred skin tumors, the presence of these NO-producing myeloid cells with suppressive activity toward T cells in vitro were required for CTL tumoricidal activity in vivo. These data indicate that myeloid cells displaying immunosuppressive activity in vitro do not inhibit the effector phase of CTL responses in vivo. Indeed, other studies have reported that splenic myeloid cells from tumor-bearing mice suppress T cell proliferation but not early effector function, such as IFN-γ expression (44, 45). Therefore, MDSCs may primarily act during the priming phase to limit tumor-specific T cell expansion. In contrast, Mϕs cocultured with MDSCs have been reported to be impaired in their ability to secrete IL-12 suggesting that MDSCs can inhibit Mϕ function (46). However, Mϕ NO production was not reduced by MDSCs in this study, which minimizes the relevance of these observations to immune evasion by ocular tumors in our model. It is very clear, however, that tumor growth induces the expansion of $CD11b^+Gr\text{-}1^+$ cells (47). Future experiments in which $Gr\text{-}1^+$ cells are eliminated in ocular tumor-bearing mice will be necessary to better define their contribution to promoting ocular tumor growth.

In our previous study, we also showed that after 7 d of E.G7-OVA growth in the a.c., mice were protected from a subsequent injection of E.G7-OVA in the skin or opposite eye (5) reproducing previous observations by Niederkorn and Streinlein (8) using P815 mastocytomas. However, in this study we observed that CTL transfer before tumor challenge in the a.c. only delayed the kinetics of ocular tumor growth. The differing results may have been due to a smaller tumor challenge (4×10^3) injected into the opposite eyes of mice with established ocular tumors and to the measurement of tumor burden only 3 d after the second eye challenge. Even though these measurements of tumor burden were below the limit of detection in the opposite eye, it is possible that tumors may have grown out over time. Our data suggest that CTLs alone directly eliminate a very limited number of E.G7-OVA tumors and require additional immune cell populations, for example Mϕs, to eliminate larger tumor burdens. Smaller tumor burdens may be controlled without the need for Mϕs. However, in larger tumor burdens, selective pressure by CTL responses in the absence of other immune effector mechanisms, such as the tumoricidal activity of activated $F4/80^+$ Mϕs, may favor the generation of tumor escape variants resistant to CTL responses, which could explain why CTL transfer on the same day as ocular tumor challenge failed to eliminate ocular tumors completely (Fig. 1).

Ocular tumor growth has been shown to induce the generation of $CD8^+$ Tregs, which inhibit the expression of delayed-type hypersensitivity responses (48). As ocular tumors ultimately completely fill the a.c. displacing the immune-suppressive AqH, another explanation for progressive ocular tumor growth is that $CD8^+$ Tregs infiltrate established ocular tumors and suppress Mϕ tumoricidal activity when AqH is lost. Additional experimentation will be required to determine whether endogenous $CD8^+FoxP3^+$ Tregs infiltrate ocular tumors and contribute to ocular tumor progression.

Not all tumor cell lines grow unabated in the a.c. of the eye, and destructive and nondestructive patterns of immune rejection of ocular tumors have been observed (35). Destructive immune responses culminating in ocular phthisis were observed when P91 tumors, a variant of P815 mastocytomas, were injected in the a.c. of BALB/c mice. This antitumor response was mediated by a T cell-mediated type IV delayed-type hypersensitivity response (49). In contrast, UV5C25 (35) and an adenovirus virus-induced tumor (Ad5E1) (50) are spontaneously eliminated from the a.c. of mice with pristine preservation of delicate ocular microanatomy. UV5C25 and Ad5E1 induce $CD8^+$ (35) and $CD4^+$ (51) T cell responses, respectively, which are required for tumor elimination. Indeed, $CD4^+$ T cell-expressed IFN-γ acts directly on Ad5E1 tumors to upregulate TRAIL-R2 to induce apoptosis (51). However, Mϕs are also required for rejection (52, 53), which is consistent with our results. The requirement for Mϕs in $CD8^+$ T cell-mediated killing of UV5C25 tumors has not been explored, but

Downloaded from http://journals.aai.org/jimmunol/article-pdf/185/11/6706/1325334/0903411.pdf by guest on 20 April 2024

based on our results a critical role for Mϕs seems plausible. Notably, although these data suggest that UV5C25 and Ad5E1 break ocular immune privilege, some immune regulation within the eye is not lost because Mϕs selectively destroy tumor cells without causing damage to innocent bystander cells. Understanding the critical factors that promote tumoricidal activity in Mϕs while controlling deleterious nonspecific tissue damage will be an exciting area of future study.

In conclusion, though CTLs can directly eliminate some tumor cells via apoptosis, their induction of tumoricidal activity in Mϕs is critical for complete elimination of established tumors. In addition to contributing to reducing tumor burden, Mϕs may eliminate tumor variants that escape detection by CTLs. Impaired effector function of Mϕs within the eye may be an evolutionary compromise to preserve vision by protecting the delicate microanatomy of the eye, which fails to regenerate from injury due to nonspecific effector mechanisms of Mϕs. However, this compromise comes at the price of impaired tumoricidal immune responses.

Acknowledgments

We thank Kelly Beatty, Stephen Harvey, Kira Lathrop, and Nancy Zurowski for excellent technical assistance and Drs. Robert Hendricks and Sidney Morris, Jr. for helpful discussions.

Disclosures

The authors have no financial conflicts of interest.

References

1. Streilein, J. W. 2003. Ocular immune privilege: therapeutic opportunities from an experiment of nature. *Nat. Rev. Immunol.* 3: 879–889.
2. Niederkorn, J. Y. 2006. See no evil, hear no evil, do no evil: the lessons of immune privilege. *Nat. Immunol.* 7: 354–359.
3. Niederkorn, J. Y. 2009. Immune escape mechanisms of intraocular tumors. *Prog. Retin. Eye Res.* 28: 329–347.
4. Niederkorn, J. Y., J. W. Streilein, and J. A. Shadduck. 1981. Deviant immune responses to allogeneic tumors injected intracamerally and subcutaneously in mice. *Invest. Ophthalmol. Vis. Sci.* 20: 355–363.
5. McKenna, K. C., and J. A. Kapp. 2006. Accumulation of immunosuppressive CD11b+ myeloid cells correlates with the failure to prevent tumor growth in the anterior chamber of the eye. *J. Immunol.* 177: 1599–1608.
6. Niederkorn, J. Y., and J. W. Streilein. 1983. Alloantigens placed into the anterior chamber of the eye induce specific suppression of delayed-type hypersensitivity but normal cytotoxic T lymphocyte and helper T lymphocyte responses. *J. Immunol.* 131: 2670–2674.
7. Ksander, B. R., and J. W. Streilein. 1989. Analysis of cytotoxic T cell responses to intracameral allogeneic tumors. *Invest. Ophthalmol. Vis. Sci.* 30: 323–329.
8. Niederkorn, J. Y., and J. W. Streilein. 1983. Intracamerally induced concomitant immunity: mice harboring progressively growing intraocular tumors are immune to spontaneous metastases and secondary tumor challenge. *J. Immunol.* 131: 2587–2594.
9. Durie, F. H., A. M. Campbell, W. R. Lee, and B. E. Damato. 1990. Analysis of lymphocytic infiltration in uveal melanoma. *Invest. Ophthalmol. Vis. Sci.* 31: 2106–2110.
10. Meecham, W. J., D. H. Char, and S. Kaleta-Michaels. 1992. Infiltrating lymphocytes and antigen expression in uveal melanoma. *Ophthalmic Res.* 24: 20–26.
11. Chen, P. W., T. Uno, and B. R. Ksander. 2006. Tumor escape mutants develop within an immune-privileged environment in the absence of T cell selection. *J. Immunol.* 177: 162–168.
12. Hallermalm, K., K. Seki, A. De Geer, B. Motyka, R. C. Bleackley, M. J. Jager, C. J. Froelich, R. Kiessling, V. Levitsky, and J. Levitskaya. 2008. Modulation of the tumor cell phenotype by IFN-gamma results in resistance of uveal melanoma cells to granule-mediated lysis by cytotoxic lymphocytes. *J. Immunol.* 180: 3766–3774.
13. Griffith, T. S., T. Brunner, S. M. Fletcher, D. R. Green, and T. A. Ferguson. 1995. Fas ligand-induced apoptosis as a mechanism of immune privilege. *Science* 270: 1189–1192.
14. Lee, H. O., J. M. Herndon, R. Barreiro, T. S. Griffith, and T. A. Ferguson. 2002. TRAIL: a mechanism of tumor surveillance in an immune privileged site. *J. Immunol.* 169: 4739–4744.
15. Hori, J., M. Wang, M. Miyashita, K. Tanemoto, H. Takahashi, T. Takemori, K. Okumura, H. Yagita, and M. Azuma. 2006. B7-H1-induced apoptosis as a mechanism of immune privilege of corneal allografts. *J. Immunol.* 177: 5928–5935.
16. Shrikant, P., and M. F. Mescher. 1999. Control of syngeneic tumor growth by activation of CD8+ T cells: efficacy is limited by migration away from the site and induction of nonresponsiveness. *J. Immunol.* 162: 2858–2866.
17. Ksander, B. R., D. C. Geer, P. W. Chen, M. L. Salgaller, P. Rubsamen, and T. G. Murray. 1998. Uveal melanomas contain antigenically specific and nonspecific infiltrating lymphocytes. *Curr. Eye Res.* 17: 165–173.
18. McKenna, K. C., K. M. Beatty, R. A. Bilonick, L. Schoenfield, K. L. Lathrop, and A. D. Singh. 2009. Activated CD11b+ CD15+ granulocytes increase in the blood of patients with uveal melanoma. *Invest. Ophthalmol. Vis. Sci.* 50: 4295–4303.
19. Staibano, S., M. Mascolo, F. Tranfa, G. Salvatore, C. Mignogna, P. Bufo, L. Nugnes, G. Bonavolontà, and G. De Rosa. 2006. Tumor infiltrating lymphocytes in uveal melanoma: a link with clinical behavior? *Int. J. Immunopathol. Pharmacol.* 19: 171–179.
20. Gabrilovich, D. I., and S. Nagaraj. 2009. Myeloid-derived suppressor cells as regulators of the immune system. *Nat. Rev. Immunol.* 9: 162–174.
21. Mäkitie, T., P. Summanen, A. Tarkkanen, and T. Kivelä. 2001. Tumor-infiltrating macrophages (CD68(+) cells) and prognosis in malignant uveal melanoma. *Invest. Ophthalmol. Vis. Sci.* 42: 1414–1421.
22. Hollenbaugh, J. A., and R. W. Dutton. 2006. IFN-gamma regulates donor CD8 T cell expansion, migration, and leads to apoptosis of cells of a solid tumor. *J. Immunol.* 177: 3004–3011.
23. Hogquist, K. A., S. C. Jameson, W. R. Heath, J. L. Howard, M. J. Bevan, and F. R. Carbone. 1994. T cell receptor antagonist peptides induce positive selection. *Cell* 76: 17–27.
24. Moore, M. W., F. R. Carbone, and M. J. Bevan. 1988. Introduction of soluble protein into the class I pathway of antigen processing and presentation. *Cell* 54: 777–785.
25. Zhang, B., N. A. Bowerman, J. K. Salama, H. Schmidt, M. T. Spiotto, A. Schietinger, P. Yu, Y. X. Fu, R. R. Weichselbaum, D. A. Rowley, et al. 2007. Induced sensitization of tumor stroma leads to eradication of established cancer by T cells. *J. Exp. Med.* 204: 49–55.
26. Darrah, P. A., D. T. Patel, P. M. De Luca, R. W. Lindsay, D. F. Davey, B. J. Flynn, S. T. Hoff, P. Andersen, S. G. Reed, S. L. Morris, et al. 2007. Multifunctional TH1 cells define a correlate of vaccine-mediated protection against *Leishmania major. Nat. Med.* 13: 843–850.
27. Hollenbaugh, J. A., J. Reome, M. Dobrzanski, and R. W. Dutton. 2004. The rate of the CD8-dependent initial reduction in tumor volume is not limited by contact-dependent perforin, Fas ligand, or TNF-mediated cytolysis. *J. Immunol.* 173: 1738–1743.
28. Takeuchi, M., P. Alard, and J. W. Streilein. 1998. TGF-β promotes immune deviation by altering accessory signals of antigen-presenting cells. *J. Immunol.* 160: 1589–1597.
29. Hu, D. E., S. O. Dyke, A. M. Moore, L. L. Thomsen, and K. M. Brindle. 2004. Tumor cell-derived nitric oxide is involved in the immune-rejection of an immunogenic murine lymphoma. *Cancer Res.* 64: 152–161.
30. Taylor, A. W. 2007. Ocular immunosuppressive microenvironment. *Chem. Immunol. Allergy* 92: 71–85.
31. Winn, H. J. 1961. Immune mechanisms in homotransplantation. II. Quantitative assay of the immunologic activity of lymphoid cells stimulated by tumor homografts. *J. Immunol.* 86: 228–239.
32. Miki, S., B. Ksander, and J. W. Streilein. 1993. Complete elimination ('cure') of progressively growing intraocular tumors by local injection of tumor-specific CD8+ T lymphocytes. *Invest. Ophthalmol. Vis. Sci.* 34: 3622–3634.
33. Barber, D. L., E. J. Wherry, D. Masopust, B. Zhu, J. P. Allison, A. H. Sharpe, G. J. Freeman, and R. Ahmed. 2006. Restoring function in exhausted CD8 T cells during chronic viral infection. *Nature* 439: 682–687.
34. Wherry, E. J., S. J. Ha, S. M. Kaech, W. N. Haining, S. Sarkar, V. Kalia, S. Subramaniam, J. N. Blattman, D. L. Barber, and R. Ahmed. 2007. Molecular signature of CD8+ T cell exhaustion during chronic viral infection. *Immunity* 27: 670–684.
35. Knisely, T. L., M. W. Luckenbach, B. J. Fischer, and J. Y. Niederkorn. 1987. Destructive and nondestructive patterns of immune rejection of syngeneic intraocular tumors. *J. Immunol.* 138: 4515–4523.
36. Taylor, A. W., D. G. Yee, and J. W. Streilein. 1998. Suppression of nitric oxide generated by inflammatory macrophages by calcitonin gene-related peptide in aqueous humor. *Invest. Ophthalmol. Vis. Sci.* 39: 1372–1378.
37. Nicholson, B., C. K. Manner, J. Kleeman, and C. L. MacLeod. 2001. Sustained nitric oxide production in macrophages requires the arginine transporter CAT2. *J. Biol. Chem.* 276: 15881–15885.
38. Bertholet, S., E. Tzeng, E. Felley-Bosco, and J. Mauël. 1999. Expression of the inducible NO synthase in human monocytic U937 cells allows high output nitric oxide production. *J. Leukoc. Biol.* 65: 50–58.
39. Mori, M. 2007. Regulation of nitric oxide synthesis and apoptosis by arginase and arginine recycling. *J. Nutr.* 137(6, Suppl 2)1616S–1620S.
40. Stickings, P., S. K. Mistry, J. L. Boucher, S. M. Morris, and J. M. Cunningham. 2002. Arginase expression and modulation of IL-1beta-induced nitric oxide generation in rat and human islets of Langerhans. *Nitric Oxide* 7: 289–296.
41. Baek, K. J., B. A. Thiel, S. Lucas, and D. J. Stuehr. 1993. Macrophage nitric oxide synthase subunits. Purification, characterization, and role of prosthetic groups and substrate in regulating their association into a dimeric enzyme. *J. Biol. Chem.* 268: 21120–21129.
42. Faunce, D. E., K. H. Sonoda, and J. Stein-Streilein. 2001. MIP-2 recruits NKT cells to the spleen during tolerance induction. *J. Immunol.* 166: 313–321.
43. Kusmartsev, S., and D. I. Gabrilovich. 2005. STAT1 signaling regulates tumor-associated macrophage-mediated T cell deletion. *J. Immunol.* 174: 4880–4891.
44. Dolcetti, L., E. Peranzoni, S. Ugel, I. Marigo, A. Fernandez Gomez, C. Mesa, M. Geilich, G. Winkels, E. Traggiai, A. Casati, et al. 2010. Hierarchy of immunosuppressive strength among myeloid-derived suppressor cell subsets is determined by GM-CSF. *Eur. J. Immunol.* 40: 22–35.

Downloaded from http://journals.aai.org/jimmunol/article-pdf/185/11/6706/1325334/0903411.pdf by guest on 20 April 2024

45. Gallina, G., L. Dolcetti, P. Serafini, C. De Santo, I. Marigo, M. P. Colombo, G. Basso, F. Brombacher, I. Borrello, P. Zanovello, et al. 2006. Tumors induce a subset of inflammatory monocytes with immunosuppressive activity on CD8+ T cells. *J. Clin. Invest.* 116: 2777–2790.
46. Sinha, P., V. K. Clements, S. K. Bunt, S. M. Albelda, and S. Ostrand-Rosenberg. 2007. Cross-talk between myeloid-derived suppressor cells and macrophages subverts tumor immunity toward a type 2 response. *J. Immunol.* 179: 977–983.
47. Youn, J. I., S. Nagaraj, M. Collazo, and D. I. Gabrilovich. 2008. Subsets of myeloid-derived suppressor cells in tumor-bearing mice. *J. Immunol.* 181: 5791–5802.
48. Streilein, J. W., and J. Y. Niederkorn. 1985. Characterization of the suppressor cell(s) responsible for anterior chamber-associated immune deviation (ACAID) induced in BALB/c mice by P815 cells. *J. Immunol.* 134: 1381–1387.
49. Niederkorn, J. Y., and P. C. Meunier. 1985. Spontaneous immune rejection of intraocular tumors in mice. *Invest. Ophthalmol. Vis. Sci.* 26: 877–884.
50. Schurmans, L. R., L. Diehl, A. T. den Boer, R. P. Sutmuller, Z. F. Boonman, J. P. Medema, E. I. van der Voort, J. Laman, C. J. Melief, M. J. Jager, and R. E. Toes. 2001. Rejection of intraocular tumors by CD4(+) T cells without induction of phthisis. *J. Immunol.* 167: 5832–5837.
51. Wang, S., Z. F. Boonman, H. C. Li, Y. He, M. J. Jager, R. E. Toes, and J. Y. Niederkorn. 2003. Role of TRAIL and IFN-gamma in CD4+ T cell-dependent tumor rejection in the anterior chamber of the eye. *J. Immunol.* 171: 2789–2796.
52. Boonman, Z. F., L. R. Schurmans, N. van Rooijen, C. J. Melief, R. E. Toes, and M. J. Jager. 2006. Macrophages are vital in spontaneous intraocular tumor eradication. Invest. *Ophthalmol. Vis. Sci.* 47: 2959–2965.
53. Dace, D. S., P. W. Chen, and J. Y. Niederkorn. 2008. CD4+ T-cell-dependent tumour rejection in an immune-privileged environment requires macrophages. *Immunology* 123: 367–377.

Downloaded from http://journals.aai.org/jimmunol/article-pdf/185/11/6706/1325334/0903411.pdf by guest on 20 April 2024